

Light-adapted electroretinograms in optic nerve hypoplasia

Caroline Chaplin · Mark S. Borchert ·
Cassandra Fink · Pamela Garcia-Filion ·
Daphne L. McCulloch

Received: 4 May 2008 / Accepted: 14 July 2009 / Published online: 11 August 2009
© Springer-Verlag 2009

Abstract The purpose of the study is to characterise retinal function using light-adapted electroretinograms (ERGs) in a series of young children with ONH, congenital dysplasia of retinal ganglion cells. ERGs were recorded with chloral hydrate sedation in 27 children with ONH (18 with bilateral and 9 with unilateral ONH, age 4–35 months) and an adult reference population ($n = 12$). Stimuli included ISCEV standard flash, oscillatory potentials (OPs) and standard flicker as well as a light-adapted luminance–response series (photopic hill). The disc diameter to disc macula (DD:DM) ratio was measured from fundus photographs. The results are eyes with ONH, classified by DD:DM, were severe (≤ 0.15 , $n = 22$), moderate ($0.16–0.30$, $n = 22$), mild ($0.31–0.35$, $n = 1$), and fellow eyes (>0.35 , $n = 9$), all had prolonged ERG implicit times and smaller i-waves than those of adults. Eyes with moderate or severe ONH also had smaller amplitudes for OPs and flicker ERGs and required stronger flashes to obtain the peak b-wave amplitude. Abnormalities of the photopic hill were a common but inconsistent feature

of ONH and were not indicative of ONH severity. Abnormalities of the photopic hill of the ERG suggest that some cases of ONH may have retinal dysfunction with specific deficits in the ON or OFF pathways of the retina. ONH is a complex and heterogeneous condition that may involve dysfunction distal to the retinal ganglion cells.

Keywords Optic nerve hypoplasia (ONH) · Light-adapted ERG · Photopic hill · Neuro-ophthalmology

Introduction

Optic nerve hypoplasia (ONH) is a non-progressive dysplasia of the retinal ganglion cell layer, which occurs during foetal development [1]. The small appearance of the optic nerves in ONH is associated with a reduced number of axons (optic nerve fibres). ONH may occur as an isolated abnormality in one or both eyes, or in association with a heterogeneous group of disorders of the brain [1–3]. The pathogenesis may involve underdevelopment or increased apoptosis of retinal ganglion cells [4]. Vision in eyes with ONH ranges from near normal to no light perception. Visual field defects, strabismus, nystagmus, high refractive errors, and deficits of brightness and colour perception are also associated [1, 2, 5–7].

C. Chaplin · D. L. McCulloch (✉)
Vision Sciences, Glasgow Caledonian University,
Glasgow, Scotland, UK
e-mail: dlmc@gcal.ac.uk

M. S. Borchert · C. Fink · P. Garcia-Filion
Childrens Hospital Los Angeles, and Keck School of
Medicine, University of Southern California,
Los Angeles, CA, USA

As ONH frequently occurs in conjunction with other malformations of the central nervous system, early diagnosis, and prognostic information is important to avoid confusion with amblyopia and to mitigate adverse outcomes associated with visual impairment, endocrine dysfunction, and developmental delay [8–13]. Reliable strategies for objective diagnosis of ONH based on the optic disc size relative to other fundus features have been devised [14–17].

Electroretinograms (ERGs) to flash stimuli are typically normal in ONH [18–20], consistent with the notion that the deficit is isolated to the retinal ganglion cells. However, ERG abnormalities have been reported in some cases of ONH, suggesting retinal dysplasia distal to the ganglion cell layer in a subset of cases [21–24].

The light-adapted flash ERGs consist of two main components, a negative a-wave generated primarily by spiking cells of the inner retina and a positive b-wave arising primarily from the middle retinal neuropile. In brief, the b-wave represents the sum of the activity generated by the ON and OFF pathways of the retina [25, 26]. The ON pathway response increases with stronger flashes and reaches a plateau for very strong flashes, while the OFF pathway response contributes to the b-wave for dim and moderate flash stimuli but is diminished and delayed for stronger flashes. Thus, the combined luminance–response function for the photopic b-wave characteristically increases in amplitude up to an optimum value then decreases to a plateau. This function has been termed the ‘photopic hill’ [27].

We have recorded standard light-adapted ERGs and plotted luminance–response functions in a cohort of young children with ONH to investigate the function of the outer and middle retinal layers in this condition.

Methods

Participants were recruited to a long-term prospective study of prenatal and clinical risk factors of ONH at Childrens Hospital Los Angeles (CHLA). Eligible children are diagnosed with ONH and referred to the study before 36 months of age. In addition to electrophysiology testing, participants have visual, developmental, neuro-radiographic, and endocrinologic evaluations and are followed annually until they

reach 5 years of age. The present study reports data from 23 consecutive participants recruited after August 2003, when the photopic ERG protocol was introduced. As it is not ethical to sedate a control population of infants, data were compared according to the severity of ONH, including fellow eyes in unilateral cases. There were insufficient fellow eyes in the original cohort, so four additional participants with unilateral ONH were added to the cohort after the consecutive series to improve the power of comparisons. Children with ONH were sedated with oral chloral hydrate (100 mg/kg) for examination, clinical electrophysiology and ocular biometry. Cycloplegia was achieved with three drops of a combination preparation (0.5% tropicamide, 0.4% phenylephrine, and 0.5% cyclopentolate). An adult reference population ($n = 12$) was tested at Glasgow Caledonian University without sedation. Adult data are reported for one eye; pupil dilation and topical anaesthesia were achieved with two drops each of Tropicamide (0.5%) and proxymetacaine (0.5%).

Approval was obtained from the appropriate ethics committees at each establishment and fulfilled the requirements of the Helsinki agreement. Signed consent was obtained prior to participation from each participant, parent or guardian, following explanation of procedure and withdrawal rights.

ONH severity

An expert neuro-ophthalmologist (MSB) assessed the horizontal diameter of the optic disc (DD) and the distance from the temporal disc margin to the centre of the macula (DM) from fundus photographs recorded during sedation. The centre of the macula was identified as the centre of the macular pigment when a foveal pit was not apparent. The temporal margin is easily identified and avoids controversy about locating the centre when discs are irregular. Four categories of ONH were defined based on the DD/DM ratio: severe (DD:DM ≤ 0.15), moderate (DD:DM 0.16–0.30), mild (DD:DM 0.31–0.35), and fellow eye (DD:DM > 0.35) [9, 10]. MSB also assessed retinal vessel appearance for tortuosity, the double ring sign and optic nerve head pallor from the photos, while blind to clinical and functional details of the patient. All adult subjects had DD:DM ratios greater than 0.35.

Electroretinography

Electroretinograms were initially recorded using a standard Burian–Allen (BA) bipolar contact lens electrode, but insertion awakened the initial participant from the light sedation; he then required re-settling. Subsequent ERGs were recorded using a Dawson, Trick, Litzkow (DTL) fibre electrode placed in the inferior cul-de-sac referenced to a skin electrode near the ipsilateral outer canthus [28]. Data from one ONH subject (two eyes) were collected using a BA electrode. A subset of adults was tested with both electrode types, demonstrating that waveforms and implicit times are similar but amplitudes recorded with the BA electrode are approximately double. Amplitude data collected with the BA electrode are excluded from quantitative comparisons.

Electroretinograms included the three ISCEV standard light-adapted tests [29]: the single flash ERG, the light-adapted oscillatory potentials (OPs) and the 30 Hz flicker ERG. We used 4 ms flashes with time-integrated (t-i) luminance of $2.55 \text{ cd}\cdot\text{s}/\text{m}^2$.¹ The ‘photopic hill’ luminance–response series was recorded for 12 flash stimuli presented in a fixed order of increasing strength from $0.01 \text{ cd}\cdot\text{s}/\text{m}^2$ to $26 \text{ cd}\cdot\text{s}/\text{m}^2$ in approximately 0.4 log unit increments. All stimuli were full-field white flashes delivered unilaterally on a full-field standard background ($25.5 \text{ cd}/\text{m}^2$) by a hand-held mini Ganzfeld (Color Burst®, Diagnosys, UK). The tested eye was held open manually and the untested eye was covered with a light excluding black patch. ERG acquisition and data processing used the Espion, E2® evoked potential system (Diagnosys, UK). All good quality sweeps accepted after manual rejection of blink artefacts were averaged for the final ERG waveforms.

Amplitude and implicit time of the ERG components for flash ERGs (a-wave, b-wave, and i-wave amplitudes and implicit times) and the individual OP amplitudes, implicit times, and the summed OP

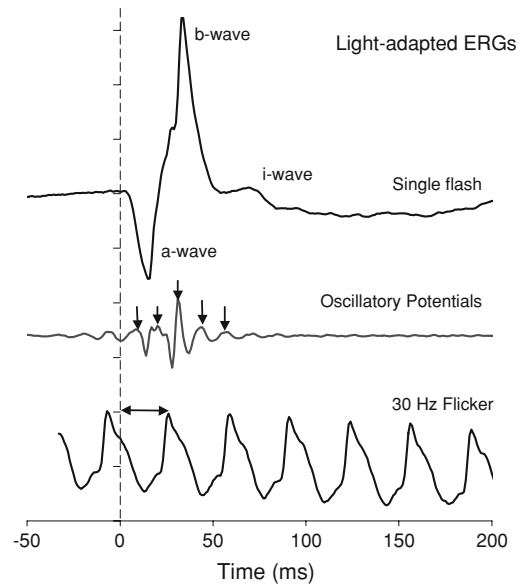
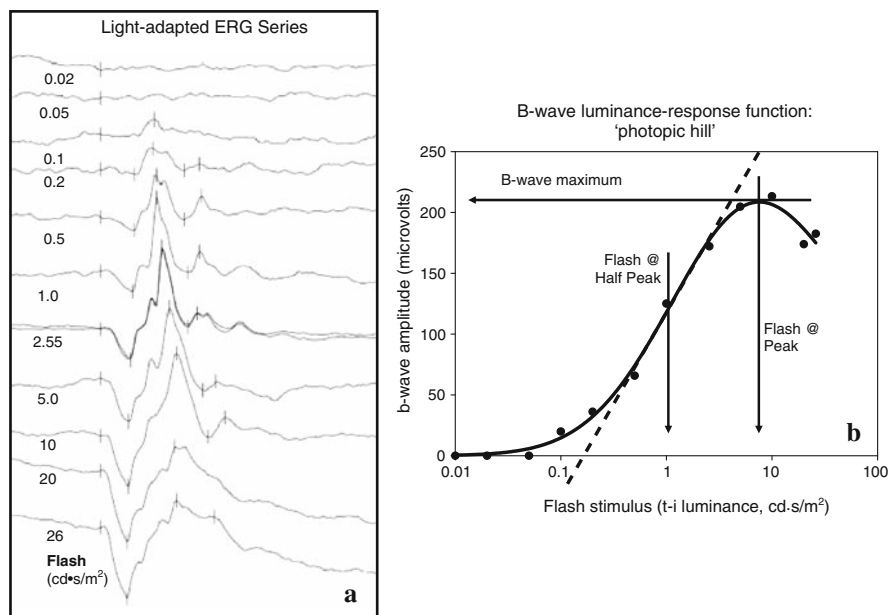


Fig. 1 ISCEV standard light-adapted ERGs for single flash (upper), OPs (middle), and 30 Hz flicker (lower) are illustrated for a right eye with moderate ONH (DD:DM = 0.21) of a 15-month-old child with unilateral ONH. Vertical arrows indicate the locations of OPI to OP5. The double arrow shows the measurement for phase (time to peak/inter-flash interval $\times 360^\circ$)

amplitudes (SOP) were measured (Fig. 1). Flicker ERG magnitude and phase were estimated from the peak-to-peak amplitude and from the position of the peaks relative to the flash onset [29, 30]. For ‘photopic hill’ analysis, b-wave amplitudes were plotted against the log of the t-i luminance of the stimuli and the curves were interpolated using the sum of a Gaussian and a Naka–Rushton function [31]. The maximal stimulus was not strong enough to define the high luminance plateau level, so plateau levels were not compared. We defined three features of the photopic hills manually from the interpolated curve: the maximum b-wave amplitude, the strength of the flash at this maximum, and on the ascending portion of the curve, the flash strength that produced half the maximum b-wave amplitude (Fig. 2) [32]. Quantitative comparisons are reported for the randomly selected eye of the adults and the left eyes of trial participants. (Comparisons were repeated for right eyes and did not differ except that there was only one fellow eye that was a right eye, so there were insufficient data to compare fellow eyes with ONH eyes for the right eyes.)

¹ This stimulus complies with the ISCEV standards for electroretinography (2004 update) and earlier standards but not the 2008 update which specifies the standard flash as $3.0 \text{ cd}\cdot\text{s}/\text{m}^2$ ($\pm 10\%$) [30]. Our stimulus is slightly weaker than the new standard.

Fig. 2 ERGs for a light-adapted luminance–response series (*left*) are plotted as a photopic hill (*right*) for the left eye with a DD:DM of 0.12 in a 17-month-old child with severe bilateral ONH. The empirical parameters measured from the interpolated curve on the right graph are the maximal B-wave amplitude, the flash producing this maximal amplitude and the flash at half the maximal b-wave amplitude



Results

Participants and success rates

A total of 27 participants [age range 17.5–153 weeks (4–35 months)] included 18 children with bilateral ONH and nine children with unilateral ONH. Bilateral cases were comprised of seven children with severe ONH, eight with moderate ONH, and three with asymmetric ONH (one moderate and one severe eye in all three). The affected eyes in unilateral cases had severe ONH ($n = 5$), moderate ONH ($n = 3$), and mild ONH ($n = 1$). The participants had the expected range of associated abnormalities: 12 had hypoplasia of the corpus callosum, three had other major cerebral malformations, five children had seizure disorders, and 19 had nystagmus. All except one child (with bilateral moderate ONH) had strabismus; 14 had esotropia; and 12 had exotropia. Ocular signs of ONH included double ring sign (41 eyes), tortuous retinal vessels (10 eyes), and pale optic nerves (temporal pallor 10 eyes, complete pallor 17 eyes). Each of these ocular signs was more frequently observed in eyes with more severe ONH ($P < 0.01$ Kendall's rank correlation).

Electroretinogram data were obtained from 53 of 54 eyes (94%) from the 27 participants with ONH. The numbers of successfully completed ERGs for each stimulus are summarised in Table 1. ERG

testing was incomplete when the infant recovered from sedation prematurely. The single eye with mild ONH was excluded from comparisons of the severity groups as were the amplitude data collected using a BA electrode.

Standard light-adapted flash ERGs

In all participants, the standard flash ERG showed the expected waveform with a negative a-wave preceding a positive b-wave and a smaller positive i-wave on the descending limb of the b-wave (Fig. 1; Table 2). The a-wave and the b-wave amplitudes did not differ among the groups of eyes (ANOVA, $P > 0.1$). Adult i-wave amplitudes were larger than those of all three groups of children's eyes: the fellow eyes, ONH moderate, and ONH severe eyes, but these eyes did not differ from each other [ANOVA $F = 33.6$, $P = 0.001$; post hoc test for differences between groups was Fisher's protected least significance difference (PLSD), $P < 0.01$].

Both a-waves and b-waves peaked earlier in the adult eyes than in all severity groups of children's eyes ($F = 13.0$ and $F = 31.1$, respectively, $P = 0.001$, Fisher PLSD, $P < 0.01$, Table 2). The implicit time for the adult i-waves was also earlier, and this reached significance for the severe and moderate ONH groups ($F = 7.9$, $P = 0.001$, Fisher PLSD, $P < 0.01$, Table 2). The i-wave implicit times in the fellow eyes

Table 1 ERGs completed for each ONH severity group, protocol, and electrode type (from 27 participants with ONH)

	Fellow eyes <i>n</i> = 8 (1) DTL (BA) ^a	Mild ONH <i>n</i> = 1 DTL	Moderate ONH <i>n</i> = 22 DTL	Severe ONH <i>n</i> = 21 (1) DTL (BA) ^a
Luminance–response function “photopic hill”	7	1	22	17
Light-adapted standard flash ERG	8 (1)	1	22	20 (1)
30 Hz flicker	5 (1)	1	20	17 (1)
Oscillatory potentials	6 (1)	1	22	16 (1)

^a Number in brackets indicates eyes tested using BA electrode. Numbers not in brackets indicate eyes tested using DTL fibre electrode

Table 2 Components of light-adapted ERGs in ONH

Light-adapted flash ERG	Adult eyes <i>n</i> = 12	Fellow eyes <i>n</i> = 8	Moderate ONH <i>n</i> = 22	Severe ONH <i>n</i> = 20
Amplitude μ V median (interquartile range)				
a-Wave	22.7 (20.5–26.5)	26.0 (23.4–29.9)	19.2 (13.8–23.9)	25.3 (18.1–30.3)
b-Wave	93.8 (85.4–103)	82.1 (78.5–92.5)	68.7 (56.5–90.3)	77.2 (66.1–98.3)
i-Wave	19.2 (7.9–20.5)	6.6* (1.8–9.6)	1.4* (0–4.3)	3.2* (2.1–6)
Implicit time ms (\pm SD)				
a-Wave	13.8 (\pm 0.8)	15.4 (\pm 1.0)*	15.4 (\pm 0.9)*	15.6 (\pm 0.8)*
b-Wave	28.3 (\pm 0.8)	32.9 (\pm 1.7)*	34.4 (\pm 2.1)*	33.6 (\pm 1.4)*
i-Wave	48.3 (\pm 1.8)	53.9 (\pm 6.6)*	58.0 (\pm 4.8)*	55.2 (\pm 5.1)*
Light-adapted OPs				
	<i>n</i> = 12	<i>n</i> = 6	<i>n</i> = 22	<i>n</i> = 16
Amplitude μ V median (interquartile range)				
OP1	17.6 (11.5–30)	14.6 (11.7–16)	8.3* (5.7–10)	8.0* (6.7–9.1)
OP2	11.4 (8.5–20)	18.5 (4.1–20)	10.7 (6.5–13)	10.6 (8.7–14)
OP3	30.8 (16–36)	21.8 (15–30)	14.0* (6.6–22)	16.3* (11–23)
OP4	14.8 (12–17)	7.8* (6.7–10)	4.9* (4.1–7.5)	6.1* (4.5–8.8)
SOP	64.5 (58–89)	41.1 (35–61)	27.1* (20–42)	37.8* (25–47)
30 Hz flicker				
	<i>n</i> = 15	<i>n</i> = 5	<i>n</i> = 20	<i>n</i> = 17
Amplitude μ V median (interquartile range)	101 (76–132)	69.8 (63–96)	66.5* (46–77)	67.4* (54–90)
Phase degrees (\pm SD)	276° (\pm 20)	313° (\pm 24)*	328° (\pm 23)*	319° (\pm 24)*

Data for the single eye with mild ONH are not shown

* Significantly different from adult values (ANOVA with Fisher’s PLSD, $P \leq 0.05$, based on left eyes)

were intermediate between adult values and those for the ONH eyes; numbers are small and these differences did not reach significance.

Light-adapted OPs

The waveform of the OPs is shown in Fig. 1. Table 2 gives the amplitudes for individual OPs and SOP, for

each group of eyes. For OP1, OP3, and SOP, the adult amplitudes were greater than those of eyes with moderate or severe ONH (separate ANOVAs, $F > 4.2$, $P < 0.01$, with Fisher PLSD $P < 0.03$). The OP1, OP3, and SOP amplitudes in the fellow eyes fell between those of the adult and the ONH eyes, but these differences do not reach statistical significance. For OP2, no difference was apparent

Table 3 Key features of the luminance–response functions for the light-adapted ERG b-waves in ONH

	Adult eyes <i>n</i> = 12	Fellow eyes <i>n</i> = 7	Moderate ONH <i>n</i> = 22	Severe ONH <i>n</i> = 17
Peak B-wave amplitude (μV) median (interquartile range)	96.5 (86–109)	101 (92–127)	82 (70–112)*	98 (85–131)
Peak flash ($\pm\text{SD}$) (t-i luminance, $\text{cd}\cdot\text{s}/\text{m}^2$)	3.6 (± 1.6)	6.5 (± 2.4)	11.1 (± 9.0)*	11.9 (± 9.1)*
Flash for the half-maximal b-wave $\pm\text{SD}$ ($\text{cd}\cdot\text{s}/\text{m}^2$)	0.81 (± 0.2)	1.09 (± 0.8)	0.89 (± 0.3)	1.12 (± 0.6)

Data for the single eye with mild ONH are not shown

* Significantly different from adult values (ANOVA with Fisher's PLSD, $P \leq 0.05$, based on left eyes)

among any of the groups ($P > 0.1$). For OP4, the adult amplitudes were greater than for each of the three groups of children's eyes (ANOVA, $F = 15.6$, $P = .0001$, with Fisher PLSD $P < 0.01$).

These data suggest that OP1 and OP3 may be selectively under-developed in the eyes with severe or moderate ONH, while OP4 demonstrates general immaturity in young eyes including the fellow eyes of those with ONH. To further evaluate the association between OPs and ONH, we set a criterion for a 'normal' OP1 of larger than $8 \mu\text{V}$, the lower limit of the adult range. The eye with mild ONH and all seven fellow eyes tested had 'normal' OP1 amplitudes giving 100% specificity for small OP1 amplitudes ($< 8 \mu\text{V}$) occurring in eyes with severe or moderate ONH. However, many of the eyes with ONH had large OP1 amplitudes ($> 8 \mu\text{V}$) so the sensitivity for detecting severe or moderate ONH based on a small OP1 was only 51% (20/39 eyes).

Flicker ERGs

Flicker ERG amplitudes were larger in the adult eyes than in eyes with severe or moderate ONH (ANOVA $F = 4.6$, $P < 0.01$, Fisher PLSD $P < 0.01$); the difference between adult eyes and ONH fellow eyes did not reach significance ($P > 0.1$). The flicker phase demonstrated lower values (advanced phase) in the adult group compared to those of the trial participants ($F = 15.1$, $P < 0.001$, Fisher PLSD $P < 0.01$). The average phase difference of 43° between adult and the children's flicker ERGs was equivalent to a 4 ms delay in the children.

Standard photopic ERGs and age

In addition to the differences with adult values as noted earlier, maturation of ERGs was expected for children within the age range tested. To examine this

maturation, two-way comparisons were made with ONH severity and age groups [4–9 months ($n = 13$), 9–18 months ($n = 24$), and 18–30 months ($n = 21$), excluding adult eyes]. The youngest group showed significant immaturity in two parameters: smaller i-waves and delayed flicker phase that are not associated with differences in DD:DM (separate two-way ANOVAs, $F > 7.5$, $P < 0.01$, with DD:DM and age groups, Fisher PLSD $P < 0.01$). None of the clinical signs, such as tortuous vessels or the associated conditions such as brain malformations were associated with a specific anomaly of the standard ERGs.

Luminance–response ERG series

A typical ERG luminance–response series for the b-wave peak amplitude (measured from the a-wave trough) is shown in Fig. 2. The majority of eyes with ONH showed this characteristic 'photopic hill' curve with a maximum b-wave and a decrease in b-wave amplitude for stronger stimuli. The values for the amplitude of the maximal b-waves in eyes with ONH ranged from supra-normal ($n = 2$) to subnormal ($n = 6$) relative to the adult values and showed no difference between the groups (Table 2). However, eight eyes (five with moderate and three with severe ONH) did not show a peak or descending phase of the photopic hill up to the maximum available flash of $26 \text{ cd}\cdot\text{s}/\text{m}^2$.

Overall the eyes with ONH required stronger flashes to generate the maximum b-wave. Specifically, t-i luminance the flash that produces the maximal b-wave was significantly higher for the ONH moderate and ONH severe eyes than for the adult group (ANOVA $F = 4.8$ $P < 0.01$, Fisher PLSD $P < 0.01$). For the ONH fellow eyes, flash stimulus at the peak was midway between the values for adult eyes and for eyes with ONH and did not differ significantly from either

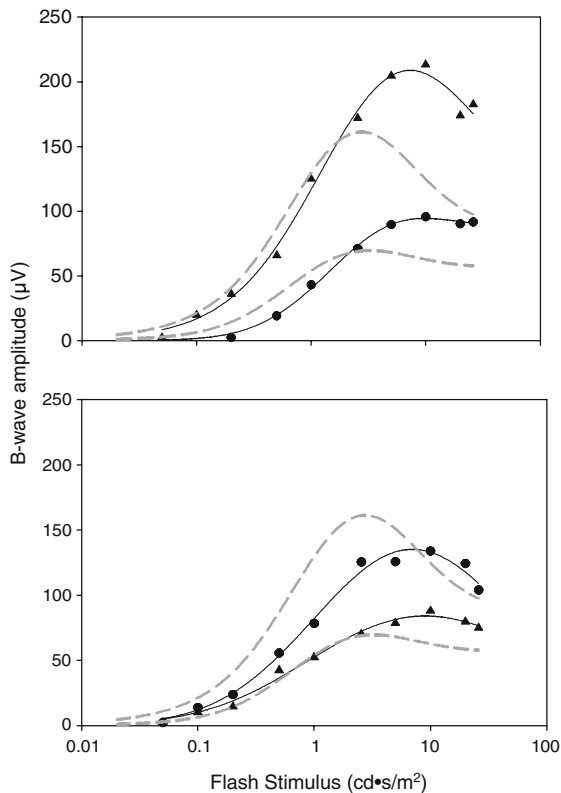


Fig. 3 Particularly large inter-ocular differences in the photopic hill curves are illustrated for two participants with severe bilateral ONH and similar DD:DM ratios in the two eyes. *Dashed lines* show the adult range. The participant in the upper plots is a 17-month-old who shows the typical ascending phase, peak and post-peak downward slope of the photopic hill in both eyes with a large asymmetry in amplitude. The lower plots are from a 19-month-old child with asymmetry in both amplitude and shape with a poorly defined ‘hill’ in the right eye

ONH group (Table 3). The t-i luminance at half of the b-wave maximum in the ascending phase of the photopic hill did not differ significantly among any of the groups, showing no evidence of differences in sensitivity for the b-waves (Table 3).

The statistical differences in the photopic hill parameters are inadequate to describe the range of the photopic hills in eyes with ONH. Four types of curve were observed: (1) entirely within the normal adult range ($n = 23$ eyes), (2) supra-normal b-wave amplitudes with normal a-waves ($n = 2$), (3) curves requiring flashes stronger than $7 \text{ cd}\cdot\text{s}/\text{m}^2$ to produce the b-wave peak or no evidence of a peak up to $26 \text{ cd}\cdot\text{s}/\text{m}^2$ ($n = 22$), and (4) diminished maximal b-wave ($<50 \mu\text{V}$, $n = 1$). Figure 3 illustrates particularly large inter-ocular differences in two individuals

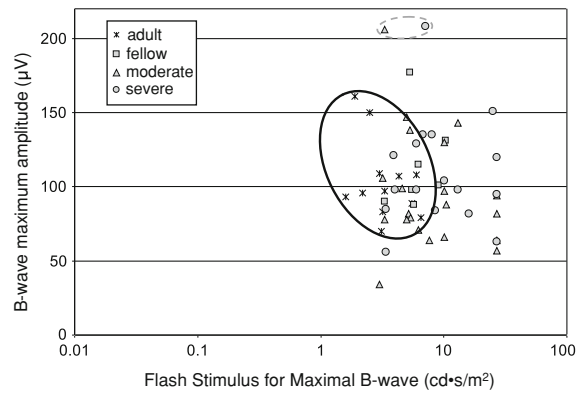


Fig. 4 The maximal b-wave amplitudes in the photopic hills are plotted against the corresponding stimulus that generates the peak. Adult values ($*, n = 12$) are enclosed within the *solid black oval* as are 17 eyes of children with ONH. The *grey dashed oval* highlights two eyes (of different participants) with supra-normal b-wave peak amplitudes relative to the adult eyes. Points to the right of the adult range depict subjects who require a greater flash luminance to generate the peak of the photopic hill

with severe bilateral ONH and similar DD:DM ratios in their two eyes. One case shows an overall difference in b-wave amplitudes between the eyes; the other has a lower amplitude and lower sensitivity in the right eye.

Characteristics of the luminance–response functions for the light-adapted b-waves were not related to the severity of ONH or to the age group within the range of children tested (two-way ANOVA, $P > 0.1$). The location of the maximum b-wave amplitudes on the luminance–response functions for all participants are shown in Fig. 4; each point represents the peak of the photopic hill for an eye, with adult values enclosed within the solid black oval. The oval also encloses 4/7 of the ONH fellow eyes, 8/22 eyes with moderate ONH, and 5/17 eyes with severe ONH. Two eyes of different participants with ONH have supra-normal b-wave peak amplitudes relative to the adult eyes. Points to the right of the adult range depict subjects who required stronger flashes to generate the peak of the photopic hill (lower sensitivity). These include two fellow eyes, nine eyes with moderate, and nine eyes with severe ONH. The remaining photopic hills have maximal b-waves for stimuli within the adult range but with peak amplitudes below the adult range.

In summary, there is surprising heterogeneity in the b-wave luminance–response curves of eyes with ONH. Abnormalities can occur uni-ocularly and do

not appear related to the severity of ONH. Additionally, ONH fellow eyes may show abnormalities; in the present series, two fellow eyes required stronger flash stimuli to reach the b-wave amplitude peak.

Discussion

The present study demonstrates that standard light-adapted ERGs are well developed in young children with ONH. The a-waves and b-waves in the children's eyes with or without ONH showed no differences in amplitude compared with adult eyes, although both components have prolonged implicit times. This is similar to data reported for typically developing children in this age range, as light-adapted ERGs mature earlier than responses from the rod system [33–35]. These data suggest that inner retinal mechanisms that generate a-waves [26], and the ON and OFF retinal pathways underlying b-wave generation are functional and developing in children's eyes with ONH, even those with severe ONH [25, 26, 29].

On the descending limb of the b-wave, the positive i-wave was smaller and later in the children's eyes than in the adult eyes and amplitude increased within the age range of children tested. The i-wave, which is associated with the OFF retinal pathways, is enhanced with damage or chemical blockage of the inner retinal spiking cells [36, 37]. Therefore, we predict that congenital ganglion cell deficits might also result in enhanced i-waves. We found no association with the severity of ONH but the numbers in this study may not provide sufficient power to detect differences when there is an interaction with the child's age.

The light-adapted 30 Hz flicker ERG also showed an immaturity in amplitude and an age-related immaturity in phase in the children's eyes regardless of ONH severity. This is expected as flicker ERGs mature later than the single flash ERGs in typically developing children [33]. The disassociation with ONH severity was also expected as proximal retinal neurons make a negligible contribution to flicker ERGs at this standard, 30 Hz, flicker frequency [38–42].

In typical children, light-adapted OPs mature unevenly; OP2 and OP5 mature before OP3 and OP4 [38, 43]. The present data show smaller OP

amplitudes in the children's eyes that reached significance for all except the early maturing OP2. OP1 is not usually reported, as it is not independent of the a-wave [44]. However, the light-adapted OP1 is the ERG component that best differentiates the adult and fellow eyes ($DD:DM > 0.35$) from the eyes with moderate or severe ONH. Large OP1 amplitudes were a consistent feature of eyes with normal $DD:DM$ values in this normal range; however, many of the eyes with ONH have OP1 amplitudes in the normal range giving low specificity for this measure (57%).

Photopic luminance–response functions for the b-wave reflect the combined contributions of the ON and OFF pathways of the retina [26]. Although many children's eyes with ONH were entirely within the range found for healthy adults, these 'photopic hills' showed a range of abnormalities. We identified two eyes with supra-normal b-waves similar to those in two previous reported cases [21, 22]. Our cases differ from previous reports in that they were asymmetric; both had bilateral asymmetric ONH with supra-normal, light-adapted b-wave amplitudes in their less affected eyes. The opposite eyes, each had normal b-wave amplitudes with poorly defined 'photopic hills' and reduced sensitivity (i.e. the luminance–response functions are shifted to the right as shown in Fig. 3, upper).

The luminance–response functions also showed several eyes with small amplitude light-adapted b-waves although none had a 'negative ERG' (a-wave \geq b-wave). Previous reports of negative ERGs in a subset of children with ONH have used scotopic ERG protocols [23, 24], not included in the present study. Some eyes with ONH failed to demonstrate the decline in amplitude for strong flash stimuli; for other eyes the entire function was shifted to the right, indicating reduced sensitivity. [We found this reduced sensitivity in 41% (9/22) eyes with moderate ONH, in 53% (9/17) with severe ONH, and in 29% (2/7) fellow eyes.] Thus, it appears that retinal dysfunction distal to the ganglion cells is inconsistent in children with ONH and can be asymmetric even when $DD:DM$ ratio is similar. This precludes the association of retinal dysfunction with a distinct pathogenesis within individuals with ONH.

Complete representation of the photopic hill, including satisfactory determination of the high luminance plateau in an adult population, requires stimulation up to 200 $cd \cdot s/m^2$. Even higher levels

might be required for infants and for eyes with dysfunction [26]. Higher flash luminance and increased testing time would require careful consideration in a young sedated population but would permit examination of the b-wave plateau values, which are not available in the present study.

Conclusion

Photopic ERG testing demonstrates that retinal dysfunction involving the photopic b-wave and OP generators is common, but variable, in eyes with ONH. Standard, photopic ERGs were recordable and of the expected morphology in all eyes with ONH; none of the cases were associated with severe retinal dysfunction or undetectable photopic ERGs. Abnormalities reflected the photopic b-wave luminance–response function (photopic hill) suggests that retinal dysfunction may selectively affect either the ON or the OFF pathways of the middle retinal layers in some, but not all, eyes with ONH. If a single stimulus has been used in cases with abnormal photopic hills, b-wave amplitudes may be either reduced or enhanced relative to adult eyes, depending on the luminance of the stimulus. ONH is a complex and heterogeneous condition; retinal dysfunction is not always isolated to the retinal ganglion cells.

Acknowledgments This research was supported in part by The One Small Voice Foundation, by NIH General Research Center (GCRG) grant (M01 RR00043) and by the Carnegie Trust for the Universities of Scotland.

References

- Lambert SR, Hoyt GS, Narahara MH (1987) Optic nerve hypoplasia. *Surv Ophthalmol* 32:1–9
- Zeki SM, Hollman AS, Dutton GN (1992) Neuroradiological features of patients with optic nerve hypoplasia. *J Pediatr Ophthalmol Strabismus* 29(2):107–112
- Tornqvist K, Ericsson A, Kallen B (2002) Optic nerve hypoplasia: risk factors and epidemiology. *Acta Ophthalmol Scand* 80(3):300–304
- Oster SF, Deiner M, Birgbauer E, Sretavan DW (2004) Ganglion cell axon pathfinding in the retina and optic nerve. *Semin Cell Dev Biol* 15(1):125–136
- Dutton GN (2004) Congenital disorders of the optic nerve: excavations and hypoplasia. *Eye* 18:1038–1048
- Billock VA, Vingrys AJ, King-Smith PE (1994) Opponent-colour detection threshold asymmetries may result from reduction of ganglion cell subpopulations. *Vis Neurosci* 11:99–109
- Heron G, Dutton GN, McCulloch DL, Stanger S Pulfrich's phenomenon in optic nerve hypoplasia. Greafe's archive for clinical and experimental ophthalmology, online
- Phillips PH, Spear C, Brodsky MC (2001) Magnetic resonance diagnosis of congenital hypopituitarism in children with optic nerve hypoplasia. *J AAPOS* 5(5):275–280
- Ahmad T, Garcia-Filion P, Borchert M, Kaufman F, Burkett L, Geffner M (2006) Endocrinological and auxological abnormalities in young children with optic nerve hypoplasia: a prospective study. *J Pediatr* 148(1):78–84
- Garcia-Filion P, Nelson M, Azen C, Geffner M, Fink C, Borchert M (2008) Neuroradiographic, endocrinological, and ophthalmic correlates of adverse developmental outcomes in children with optic nerve hypoplasia. *Pediatrics* 121(3):e653–e659
- Lempert P (2000) Optic nerve hypoplasia and small eyes in presumed amblyopia. *J AAPOS* 4(5):258–266
- Borchert M, Garcia-Filion P The syndrome of optic nerve hypoplasia *Current neurology and neuroscience reports* 8 5 395–403 Sep 2008
- Taylor D (2007) Developmental abnormalities of the optic nerve and chiasm. *Eye* 21(10):1271–1284
- Alvarez E, Wakakura M, Khan Z, Dutton GN (1988) The disc-macula distance to disc diameter ratio: a new test for confirming optic nerve hypoplasia in young children. *J Pediatr Ophthalmol Strabismus* 25(3):151–154
- Barr DB, Weir CR, Purdie AT (1999) An appraisal of the disc-macula distance to disc diameter ratio in the assessment of optic disc size. *Ophthalmic Physiol Opt* 19(5):365–375
- Zeki SM, Dutton GN (1990) Optic nerve hypoplasia in children. *Br J Ophthalmol* 74:300–304
- Borchert MS, McCulloch DL, Rother C, Stout AU (1995) Clinical assessment, optic disk measurements, and visual-evoked potential in optic nerve hypoplasia. *Am J Ophthalmol* 120:605–612
- Francois J, Rouck AD (1976) Electroretinographical study of the hypoplasia of the optic nerve. *Ophthalmologica* 172:308–330
- Brecelj J, Stirn-Kranjc B (2004) Visual electrophysiology screening in diagnosing infants with congenital nystagmus. *Clin Neurophysiol* 115(2):461–470
- McCulloch DL, Garcia-Filion P, van Boemel GB, Borchert MS (2007) Retinal function in children with optic nerve hypoplasia: electroretinograms to large patterns and photopic flash. *Eye* 21(6):712–720
- Sprague JB, Wilson WB (1981) Electrophysiologic findings in bilateral optic nerve hypoplasia. *Arch Ophthalmol* 99(9):1028
- Kriss A, Russell-Eggitt I (1992) Electrophysiological assessment of visual pathway function in infants. *Eye* 6:145–153
- Cibis GW, Fitzgerald KM (1994) Optic nerve hypoplasia in association with brain anomalies and an abnormal electroretinogram. *Doc Ophthalmol* 86:11–22
- Janaky M, Deak A, Pelle Z, Benedek G (1994) Electrophysiologic alterations in patients with optic nerve hypoplasia. *Doc Ophthalmol* 86:247–257

25. Sieving PA, Murayama K, Naarendorp F (1994) Push-pull model of the primate photopic electroretinogram: a role for hyperpolarizing neurons in shaping the b-wave. *Vis Neurosci* 11:519–532
26. Ueno S, Kondo M, Niwa Y, Terasaki H, Miyake Y (2004) Luminance dependence of neural components that underlies the primate electroretinogram. *Invest Ophthalmol Vis Sci* 45:1033–1040
27. Wali N, Leguire LE (1992) The photopic hill: A new phenomenon of the light adapted electroretinogram. *Doc Ophthalmol* 80(4):1573–2622
28. McCulloch DL, van Boemel GB, Borchert MS (1998) Comparison of corneal, conjunctival and skin electrodes for pattern electroretinograms. *Doc Ophthalmol* 94:327–340
29. Marmor MF, Holder GE, Seeliger MW, Yamamoto S (2004) Standard for clinical electroretinography (2004 update). *Doc Ophthalmol* 108:107–114
30. Marmor MF, Fulton AB, Holder GE, Miyake Y, Brigell M, Bach M (2009) Standard for clinical electroretinography (2008 update). *Doc Ophthalmol* 118:69–77
31. Hamilton R, Bees MA, Chaplin CA, McCulloch DL (2007) The luminance-response function of the human photopic electroretinogram: a mathematical model. *Vis Res* 47(23):2968–2972
32. Rufiange M, Dassa J, Dembinska O, Koenekoop RK, Little JM, Polomeno RC, Dumont M, Chemtob S, Lachapelle P (2003) The photopic ERG luminance-response function (photopic hill): method of analysis and clinical application. *Vision Res* 43(12):1405–1412
33. Westall CA, Pantou CM, Levin AV (1999) Time courses for maturation of electroretinogram responses from infancy to adulthood. *Doc Ophthalmol* 96(4):355–379
34. Fulton AB, Hansen RM, Westall CA (2003) Development of ERG responses: the ISCEV standard rod, maximal and cone responses in normal subjects. *Doc Ophthalmol* 107:235–241
35. Hansen RM, Fulton AB (2005) Development of the cone ERG in infants. *Invest Ophthalmol Vis Sci* 46(9):3458–3462
36. Viswanathan S, Frishman LJ, Robson JG, Harwerth RS, Smith ELIII (1999) The photopic negative response of the macaque electroretinogram: reduction by experimental glaucoma. *Invest Ophthalmol Vis Sci* 40(6):1124–1136
37. Rangaswamy NV, Shirato S, Kaneko M, Digby BI, Robson JG, Frishman LJ (2007) Effects of spectral characteristics of Ganzfeld stimuli on the photopic negative response (PhNR) of the ERG. *Invest Ophthalmol Vis Sci* 48(10):4818–4828
38. Viswanathan S, Frishman LJ, Robson JG (2002) Inner-retinal contributions to the photopic sinusoidal flicker electroretinogram of macaques. *Doc Ophthalmol* 105:223–242
39. Bush RA, Sieving PA (1996) Inner retinal contributions to the primate photopic fast flicker electroretinogram. *J Opt Soc Am* 13(3):557–565
40. Peachey NS, Alexander KR, Derlacki DJ, Fishman GA (1992) Light adaptation, rods, and the human cone flicker ERG. *Vis Neurosci* 8(2):145–150
41. Usui T, Kremers J, Sharpe LT, Zrenner E (1998) Response phase of the flicker electroretinogram (ERG) is influenced by cone excitation strength. *Vis Res* 38:3247–3251
42. Kondo M, Sieving PA (2001) Primate photopic sine-wave flicker ERG: vector modelling analysis of component origins using glutamate analogs. *Invest Ophthalmol Vis Sci* 42(1):305–312
43. Moskowitz A, Hansen RM, Fulton AB (2005) ERG oscillatory potentials in infants. *Doc Ophthalmol* 110:265–270
44. Bui BV, Armitage JA, Vingrys AJ (2002) Extraction and modelling of oscillatory potentials. *Doc Ophthalmol* 104(1):7–36